

FreeFEM++ Implementation of a Shell Model Described by the Intrinsic Geometry via the Oriented Distance Function

Vittorio Sansalone ^{*†} and John Cagnol ^{‡§}

October 8, 2006

Abstract

A shell can be described via the oriented distance function, which provides a natural and simple tool to describe the geometric properties of a set and of its boundary. The advantage of this approach is the total absence of Christoffel symbols. This description is well suited for the area of smart systems, where the adaptation of the existing techniques of control theory is made easier. We shall present the implementation in FreeFEM++ of the intrinsic geometric operators and of the mechanical model, showing a test case representing the free vibrations of a circular cylinder.

Keywords: Shells; Numerical libraries; FreeFEM++; Simulation; Intrinsic Modeling.

1 Introduction

A shell is a continuous three-dimensional object of which one dimension is small compared to the other two. The small dimension is called the thickness. While the object is three-dimensional, one usually takes advantage of its small thickness to obtain a two-dimensional model based on the middle surface (or mid-surface). As a consequence, shell theory is linked to the representation of surfaces, which can be done in several ways.

The most widespread approaches to describe a shell (or the mid-surface thereof) refer to the pioneering work of Kirchhoff [1] and Love [2]. We refer to [3] and references therein, for further details.

Another way to describe a shell is via the oriented distance function (also called signed distance function) that provides a natural and simple tool to describe the geometric properties of a set and of its boundary. The advantage of this approach is the total absence of Christoffel symbols. The pioneers of this approach were Michel Delfour and Jean-Paul Zolésio. An overview of this method is described in Section 2.

The goal of this article is to show the numerical implementation of the shell model, formulated in the language of intrinsic modeling, in the FreeFEM++ environment (Section 3). As a case study we present the analysis of the free vibrations of a circular cylinder.

2 Intrinsic Geometric Modeling

We here include a brief discussion of the oriented distance function (also known as signed distance function). We refer to [4, 5] for more details.

^{*}Laboratoire de Biomécanique et Biomatériaux Ostéo-Articulaires, CNRS UMR 7052 (Lab. de Mécanique Physique), Faculté des Sciences et Technologie, Université Paris XII - Val de Marne, 94010 Créteil Cedex, France.

[†]E-mail: vittorio.sansalone@univ-paris12.fr

[‡]Pôle Universitaire Léonard de Vinci, ESILV, DER-CS, 92916 Paris La Défense Cedex, France.

[§]E-mail: john.cagnol@devinci.fr

2.1 The Oriented Distance Function

Consider a domain $\mathcal{O} \subset \mathbb{R}^3$ whose nonempty boundary $\partial\mathcal{O}$ is a C^1 two-dimensional sub-manifold of \mathbb{R}^3 . Define the oriented (or signed) distance function to \mathcal{O} as

$$b(x) = d_{\mathcal{O}}(x) - d_{\mathbb{R}^3 \setminus \mathcal{O}}(x) \quad (1)$$

where d is the Euclidean distance from the point x to the domain \mathcal{O} . In other words, $b(x)$ is simply the positive or negative distance to the boundary $\partial\mathcal{O}$, depending on if we are outside or inside the domain \mathcal{O} . It can be shown that for every $x \in \partial\mathcal{O}$, there exists a neighborhood where the function $\nabla b = \nu$, the unit outward external normal to $\partial\mathcal{O}$ [5].

Consider a subset $\Gamma \subseteq \partial\mathcal{O}$ which will eventually become the mid-surface of our shell. We define the projection $p(x)$ of a point x onto Γ as $p(x) = x - b(x)\nabla b(x)$. Then, we define a shell \mathcal{S}_h of thickness h as

$$\mathcal{S}_h(\Gamma) \equiv \{x \in \mathbb{R}^3 : p(x) \in \Gamma, |b(x)| < h/2\} \quad (2)$$

A natural curvilinear coordinate system (X, z) is thus induced on the shell \mathcal{S}_h , where the coordinate vector X gives the position of a point on the mid-surface Γ , and $z \in (-\frac{h}{2}, \frac{h}{2})$ gives the vertical (normal) distance from the mid-surface. Using this notation, we also define the ‘‘flow mapping’’ $T_z(X)$ as

$$T_z(X) = X + z\nabla b(X) \quad (3)$$

for all X and z in \mathcal{S}_h . This allows us to reconstruct the action at a given height z of the shell, once we know the action of the mid-surface Γ . Define as Γ^z the surface $T_z(\Gamma)$ at the ‘altitude’ z . Then, one can also describe the shell \mathcal{S}_h as

$$\mathcal{S}_h = \bigcup_{z=-h/2}^{h/2} \Gamma_z$$

The curvatures of the shell will be denoted H and K . These can be reconstructed from the boundary distance function $b(x)$ by noting that at any point (X, z) , the matrix D^2b has eigenvalues 0, λ_1 , λ_2 . The curvatures are then given by $\text{tr}(D^2b) = 2H = \lambda_1 + \lambda_2$ and $K = \lambda_1\lambda_2$.

2.2 Tangential Differential Calculus

Next, we mention briefly some useful aspects of the tangential differential calculus. Given $f \in C^1(\Gamma)$, we define the tangential gradient ∇_{Γ} of the scalar function f by means of the projection as

$$\nabla_{\Gamma} f \equiv \nabla(f \circ p)(x)|_{\Gamma} \quad (4a)$$

This notion of the tangential gradient is equivalent to the classical definition using an extension F of f in the neighborhood of Γ , *i.e.* $\nabla_{\Gamma} f = \nabla F|_{\Gamma} - \frac{\partial F}{\partial \nu} \nu$ [5]. Following the same idea we can define the tangential Jacobian matrix of a vector function $v \in C^1(\Gamma)^3$ as

$$D_{\Gamma} v \equiv D(v \circ p)|_{\Gamma} \text{ or } (D_{\Gamma} v)_{ij} = (\nabla_{\Gamma} v_i)_j \quad (4b)$$

the tangential divergence as

$$\text{div}_{\Gamma} v \equiv \text{div}(v \circ p)|_{\Gamma} \quad (4c)$$

the Hessian $D_{\Gamma}^2 f$ of $f \in C^2(\Gamma)$ as

$$D_{\Gamma}^2 f = D_{\Gamma}(\nabla_{\Gamma} f) \quad (4d)$$

the Laplace-Beltrami operator of $f \in C^2(\Gamma)$ as

$$\Delta_{\Gamma} f \equiv \text{div}_{\Gamma}(\nabla_{\Gamma} f) = \Delta(f \circ p)|_{\Gamma} \quad (4e)$$

the tangential linear strain tensor of elasticity as

$$\varepsilon_{\Gamma}(v) \equiv \frac{1}{2}(D_{\Gamma} v + {}^*D_{\Gamma} v) = \varepsilon(v \circ p)|_{\Gamma} \quad (4f)$$

and the tangential vectorial divergence of a second-order tensor A as

$$\operatorname{div}_\Gamma A \equiv \operatorname{div}(A \circ p)|_\Gamma = \operatorname{div}_\Gamma A_i \quad (4g)$$

Finally, from [5, 4] we have that

$$\langle \nabla_\Gamma w, \nabla b \rangle = 0, \quad D_\Gamma v \nabla b = 0 \quad (5)$$

by definition for any scalar w and vector v . In addition, if we consider a purely tangent vector $v = v_\Gamma$, *i.e.* $\langle v_\Gamma, \nabla b \rangle = 0$, we can take the tangential gradient of both sides of this expression and derive the following useful formula

$$D^2 b v_\Gamma + {}^* D_\Gamma v_\Gamma \nabla b = 0 \quad (6)$$

Throughout this paper the conventions of [6] concerning tensors are used. For instance, we will make no distinction between a second-order tensor or a matrix, nor will we make a distinction between a first-order tensor and a vector. Consequently we will not distinguish simple contraction and multiplication. Finally, the notation $\partial_t \varphi$ is used to denote the partial derivative of φ with respect to the time variable, and the notation $A \cdot \cdot B$ denotes the double contraction of two matrices – *i.e.* $A \cdot \cdot B = \operatorname{tr}(AB)$

2.3 More Tangential Operators and Spaces

Let \mathbf{e} be a vector function, we note e_Γ and w the tangential component of \mathbf{e} and its algebraic magnitude on the normal part respectively, *i.e.*

$$w = \langle \mathbf{e}, \nabla b \rangle \quad (7a)$$

$$e_\Gamma = \mathbf{e} - w \nabla b \quad (7b)$$

Vector function \mathbf{e} will physically represent the displacement of the mid-surface, its components e_Γ and w will represent the in-place displacement and the normal deflection respectively. Following the definitions introduced in [7], we will use the subsequent notations.

Definition 1 *Let w be a scalar and u a vector. We define the following operators:*

$$\begin{aligned} C_\Gamma u &= \frac{1}{2}(D^2 b {}^* D_\Gamma u + D_\Gamma u D^2 b) \\ C'_\Gamma u &= \frac{1}{2}({}^* D_\Gamma u D^2 b + D^2 b D_\Gamma u) \\ F_\Gamma w &= \frac{1}{2}((\nabla b \otimes \nabla_\Gamma w) + (\nabla_\Gamma w \otimes \nabla b)) \\ G_\Gamma w &= \frac{1}{2}((\nabla b \otimes \nabla_\Gamma w) D^2 b + D^2 b (\nabla_\Gamma w \otimes \nabla b)) \\ V_\Gamma u &= \frac{1}{2}((D^2 b u) \otimes \nabla b + \nabla b \otimes (D^2 b u)) \\ S_\Gamma w &= \frac{1}{2}(D_\Gamma^2 w + {}^* D_\Gamma^2 w) \end{aligned}$$

$C_\Gamma, C'_\Gamma, F_\Gamma$ and G_Γ are 1st-order tangential operators, V_Γ is a zero-order tangential operator, and S_Γ is the symmetrization of the Hessian (which is not symmetric in the tangential calculus [5]).

3 Numerical simulations

We implemented the shell model in FreeFEM++, [8] an open source software able to deal with a large class of mechanical problems governed by partial differential equations.

FreeFem++ has an advanced automatic mesh generator and a general purpose elliptic solver. Moreover, it easily allows for dealing with hyperbolic and parabolic problems. FreeFEM++ provides a high level language and macro expansion capabilities, by which it is possible to describe even complex problems and a quick specification of any system of partial differential equations.

3.1 Some numerical insights

A limitation of FreeFEM++ concerns the available types of finite element. In particular, only lagrangean FE are provided by default.

This class of FE is only C^0 , while in the weak form of our shell model at the least C^1 is required. Even if it is possible to implement new FE classes in FreeFEM++, this requires additional work and an in-depth knowledge of its data structures. We decided not to deal with this issue and to use the FE classes already available, modifying our formulation in order to reduce the continuity requirements.

C^1 continuity is required in the bilaplacian-like operators involving the normal deflection w , namely operator $S_\Gamma w$ and few other contributions in the energy involving $\Delta_\Gamma w$.

We introduce a new independent vector field φ describing the rotation of the mid surface of the shell, related to the normal deflection w by:

$$\varphi \equiv \nabla_\Gamma w \quad (8)$$

With this position, we can rewrite some of the differential operators appearing in our model as:

$$S_\Gamma w \equiv \varepsilon_\Gamma \varphi \quad , \quad G_\Gamma w \equiv V_\Gamma \varphi \quad , \quad \Delta_\Gamma w \equiv \operatorname{div}_\Gamma \varphi \quad (9)$$

Equation (8) is a constraint which must be suitably imposed. We tested few possibilities (penalty functions, least square method), and among them the most effective came out to be a Lagrangean multiplier technique. In this setting, the constraint above is imposed as:

$$\int_\Gamma \lambda \cdot (\varphi - \nabla_\Gamma w) \quad (10)$$

which, in the weak form of the energy, reads:

$$\int_\Gamma \lambda \cdot (\tilde{\varphi} - \nabla_\Gamma \tilde{w}) + \tilde{\lambda} \cdot (\varphi - \nabla_\Gamma w) \quad (11)$$

The lagrangean multiplier λ is the reaction responsible for maintaining the constraint and is related to the shear stress, so giving our model a mixed formulation.

3.2 Test case: Circular cylinder

As a case study we considered a circular cylinder (radius $R = 2.0$, thickness $th = 0.01$), subjected to an applied radial displacement to one end, the other being left free. In the following, we will refer to ζ as an abscissa running along the axis of the cylinder, and to θ as an abscissa running in the circumferential direction. In view of the symmetry conditions, we studied only a quarter of the cylinder, applying suitable boundary conditions in order to recover the periodicity.

Numerical results are perfectly in agreement with the exact solution [9]. On the top of fig. 2 the lateral radial displacement w of the wall of the cylinder at $\theta = \pi/4$ is plotted along the ζ abscissa: curves obtained using meshes labeled $2n$ and *split* follow exactly the exact solution, but also that obtained with mesh n is in quite good agreement. In the same picture the wave length of oscillations is also pointed out: again the numerical value is in very good agreement with the theoretical one ($w.l. = 2 * 0.586$).

Finally, on the bottom of the figure the contour map of w related to mesh *split* is shown (continuous black lines indicate $w = 0$).

The deformed configuration obtained from this analysis has been used as initial condition for studying the lateral oscillations of the cylinder (pure aluminum is again considered as target material). Figure 3 shows some snapshots of the lateral displacement w (mesh $3n$).

The time integration scheme used in our calculations is the Constant Average Acceleration (CAA) method, a variant of the Newmark's family based on the hypothesis that the acceleration in the time step is constant and equal to the average value between the initial and final time.

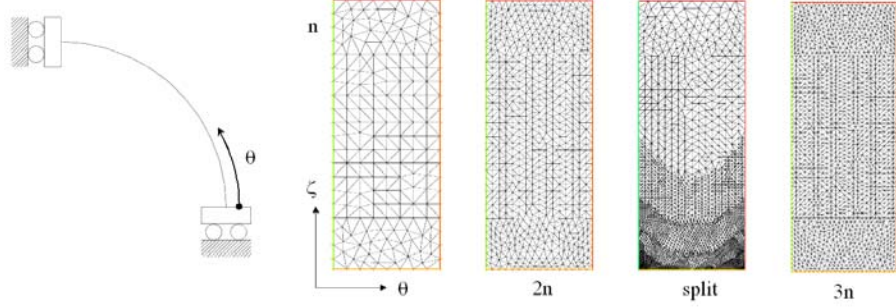


Figure 1: Left: sketch of geometry and boundary conditions. Right: Different meshes used in the simulations.

In general, for a displacement based problem, Newmark's time integration scheme is based on the following time interpolation for the displacement u and the velocity \dot{u} :

$$\begin{aligned}\dot{u}_{t+1} &= \dot{u}_t + ((1 - \delta) \ddot{u}_t + \delta \ddot{u}_{t+1}) \Delta t \\ u_{t+1} &= u_t + \dot{u}_t \Delta t + \left(\frac{1}{2} - \alpha\right) \ddot{u}_t + \alpha \ddot{u}_{t+1}) \Delta t\end{aligned}\quad (12)$$

where \ddot{u} is the acceleration.¹ This assumption leads to the iterative procedure:

$$\begin{aligned}\left(\frac{1}{\alpha \Delta t^2} M + \frac{\delta}{\alpha \Delta t} D + K\right) u_{t+1} &= p_{t+1} \\ &+ M \left(\frac{1}{\alpha \Delta t^2} u_t + \frac{1}{\alpha \Delta t} \dot{u}_t + \left(\frac{1}{2\alpha} - 1\right) \ddot{u}_t\right) \\ &+ D \left(\frac{\delta}{\alpha \Delta t} u_t + \left(\frac{\delta}{\alpha} - 1\right) \dot{u}_t + \left(\frac{\delta}{\alpha} - 2\right) \frac{\Delta t}{2} \ddot{u}_t\right) \\ \dot{u}_{t+1} &= \dot{u}_t + (1 - \delta) \Delta t \ddot{u}_t + \delta \Delta t \ddot{u}_{t+1} \\ \ddot{u}_{t+1} &= \frac{1}{\alpha \Delta t^2} (u_{t+1} - u_t) - \frac{1}{\alpha \Delta t} \dot{u}_t - \left(\frac{1}{2\alpha} - 1\right) \ddot{u}_t\end{aligned}$$

where M , D , and K are the mass, damping, and stiffness matrix, respectively. α and δ are parameters which can be tuned in order to obtain the desired convergence and accuracy of the scheme (for the CAA scheme: $\alpha = 0.25$ and $\delta = 0.5$). Moreover, since we consider free oscillations, in our case $D = 0$ and $p = 0$.

References

- [1] G. Kirchhoff. *Vorlesungen uber Mathematische Physik*. Mechanik, Leipzig, 1876.
- [2] A. E. H. Love. *The Mathematical Theory of Elasticity*. Cambridge University Press, 1934.
- [3] Michel Bernadou and Jean-Marie Boisserie. *The finite element method in thin shell theory*, volume 1 of *Progress in Scientific Computing*. Birkhäuser Boston, Mass., 1982.
- [4] Michel C. Delfour and Jean-Paul Zolésio. Differential equations for linear shells: comparison between intrinsic and classical models. In *Advances in mathematical sciences: CRM's 25 years (Montreal, PQ, 1994)*, volume 11 of *CRM Proc. Lecture Notes*, pages 41–124. Amer. Math. Soc., Providence, RI, 1997.

¹In our case, similar assumptions clearly hold for each field involved in the analysis: the formal expression above is unchanged if one think of u as the entire set of unknown fields: $u \equiv \{e_\Gamma, w, \varphi, \lambda\}$.

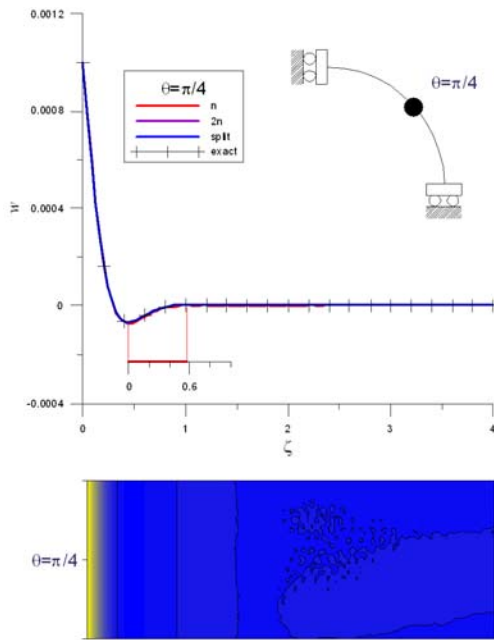


Figure 2: Radial displacement. Top: section at $\theta = \pi/4$. Bottom: contour map (continuous black lines indicate $w = 0$).

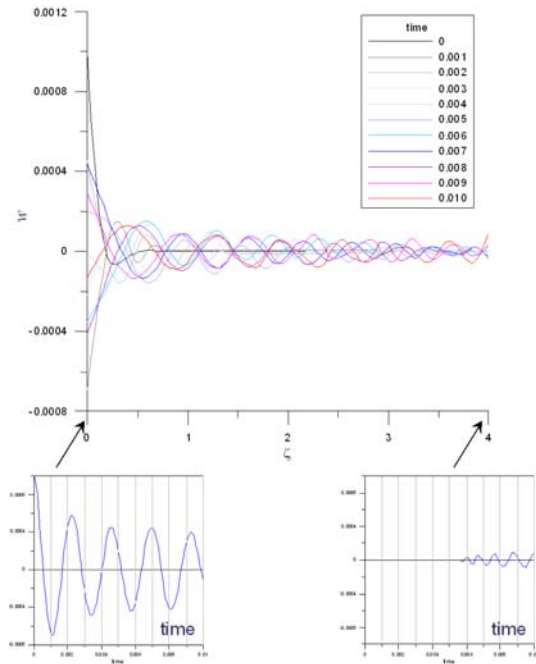


Figure 3: Top: lateral oscillations of the cylinder at $\theta = \pi/4$. Bottom panels: time evolution of w at the ends of the cylinder.

- [5] Michel C. Delfour and Jean-Paul Zolésio. *Intrinsic differential geometry and theory of thin shells*. to appear, 200x.
- [6] P. Germain. *Mécanique*, volume 1. Ecole Polytechnique, 1986.
- [7] John Cagnol, Irena Lasiecka, Catherine Lebedzik, and Jean-Paul Zolésio. Uniform stability in structural acoustic models with flexible curved walls. *J. Differential Equations*, 186(1):88–121, 2002.
- [8] Frédéric Hecht, Olivier Pironneau, Antoine Le Hyaric, and Koji Ohtsuka. Freefem++. <http://www.freefem.org/ff++/>.
- [9] Stephen P. Timoshenko and S. Woinowsky-Krieger. *Theory of Plates and Shells*. McGraw-Hill, New York, NY, 1959.